PROCEEDINGS OF SCIENCE

Measurements of $B \to DK^{(*)}$ decays to constrain the CKM unitarity triangle angle γ at LHCb

Andrew Powell[*] **for the LHCb collaboration**
University of Oxford
E-mail: a.powell1@physics.ox.ac.uk

The LHCb experiment is a general purpose forward spectrometer operating at the Large Hadron Collider, optimised for the study of B and D hadrons. The experiment collected 1.0 fb^{-1} of integrated luminosity during 2011 data taking, accumulating unprecedented samples of B hadron decays to final states involving charmed hadrons. These decays offer many complementary measurements of CP violation, in particular measurements which are sensitive to the angle γ of the CKM-unitarity triangle. We present here several world best measurements of these decays.

36th International Conference on High Energy Physics,
July 4-11, 2012
Melbourne, Australia

[*]Speaker.

PoS(ICHEP2012)360

1. Introduction

Of the three angles comprising the CKM-unitarity triangle, γ remains the least experimentally constrained. The current world average of this CP-violating parameter, taken from direct measurements, is found to be $(62 \pm 12)^\circ$ [1]. A precision measurement of this angle is highly desirable in its own right, since it is one of the eighteen arbitrary parameters of the Standard Model [2]. However, further motivation for such a measurement comes from the fact that the angle γ is the only CP-violating parameter that can be measured unambiguously via both tree- and loop-level b-decays. While loop-level processes are sensitive to possible New Physics (NP) contributions, tree-level processes are considered immune. Consequently a comparison of γ measurements made in these two types of decay constitutes a powerful search for NP. Such a series of measurements form an integral part to the LHCb physics programme [3].

These proceedings describe some of the first steps performed at LHCb towards a tree-level measurement of γ. While no determination of γ is presented, measurements of several interesting auxiliary parameters are given. These analyses have been performed using the experiments first 1.0 fb^{-1} of data recorded at $\sqrt{s} = 7$ TeV. Following a brief description of the γ extraction methodology, sections 3 and 4 present results utilising two time-independent techniques; the GLW and ADS methods, respectively. Finally section 5 describes the status of performing a time-dependent measurement of γ with the mode $B_s \to D_s K$.

2. Tree-level γ Methodology

The angle γ is defined as the relative phase-difference between $b \to u$ and $b \to c$ quark transitions. Access to this phase is made possible through the interference between two diagrams involving $b \to u\bar{c}s$ and $b \to c\bar{u}s$ processes. Considering all possible flavours of the accompanying spectator quark, q, one finds two distinct sets of tree-level decay processes involving a single D meson[1]. These are summarised in Table 1.

q	$b \to u\bar{c}s$	$b \to c\bar{u}s$
$\{u,\ d\}$	$B_q \to \overline{D^0}\, X_s$	$B_q \to D^0\, X_s$
s	$B_s^0 \to D_s\, X_s$	$\overline{B^0}_s \to D_s\, X_s$

Table 1: Tree-level processes sensitive to the CKM angle γ.

The quantity X_s is a final state with quantum numbers equivalent to that of a $K^\pm$. In the case of $q = \{u,\ d\}$, the necessary interference occurs when both the D^0 and $\overline{D^0}$ decay to a common final state. However for $q = s$, the interference occurs via $B_s^0 - \overline{B^0}_s$ mixing. Consequently, in order to extract γ one can either considering the time-integrated rates of the former set of modes, or perform a time-dependent analysis with the latter.

[1] Here and subsequently, D will denote both a D^0 and $\overline{D^0}$.

3. Time-Independent Measurements : GLW Method

A variety of time-integrated methods have been proposed in the literature, dependent on the D final state considered. The GLW technique considers CP eigenstates, D_{CP}, such as K^+K^- and $\pi^+\pi^-$ [4, 5]. Two such analyses have been performed at LHCb, utilising these final states in conjunction with the decay processes $B^\pm \to DX_s^\pm$. Analysis (A) considers a single bachelor track, $X_s^\pm = K^\pm$, while the analysis (B) considers the multi-body final state $X_s^\pm = K^\pm\pi^+\pi^-$. In both analyses two γ dependent observables are measured. They are the average partial width

$$R_{CP^+} = 2\frac{\Gamma(B^- \to D_{CP^+}X_s^-) + \Gamma(B^+ \to D_{CP^+}X_s^+)}{\Gamma(B^- \to D^0 X_s^-) + \Gamma(B^+ \to \overline{D^0} X_s^+)}, \tag{3.1}$$

and the CP asymmetry

$$A_{CP^+} = \frac{\Gamma(B^- \to D_{CP^+}X_s^-) - \Gamma(B^+ \to D_{CP^+}X_s^+)}{\Gamma(B^- \to D_{CP^+}X_s^-) + \Gamma(B^+ \to D_{CP^+}X_s^+)}. \tag{3.2}$$

It is important to note that, due to strong interaction processes within the $X_s^\pm = K^\pm\pi^+\pi^-$ final state, the values of these observables are expected to differ between analysis (A) and (B), respectively.

Both analyses utilise a multi-variant technique in order to discriminate signal from combinatoric background. Analysis (A) uses a Boosted Decision Tree algorithm, while analysis (B) implements a neural network through the NeuroBayes® software package. In each case, the discriminant is trained to isolate both the signal $B^\pm \to DX_s^\pm$ and its reflection mode $B^\pm \to DX_d^\pm$, where $X_d^\pm$ is either $\pi^\pm$ or $\pi^\pm\pi^+\pi^-$, respectively. In addition to the multi-variant output response, requirements are also imposed on the flight distance of the D in order to suppress contributions from $B^\pm$ decays not containing a D meson. The candidates selected in each analysis are then divided into four mutually-exclusive sub-samples according to:

1. the charge of the parent B-meson;
2. the Particle Identification (PID) information of the tracks associated with the D meson in order to isolate $[K^+K^-]_D$ and $[\pi^+\pi^-]_D$ enhanced samples;
3. the PID information of the track(s) not associated with the D meson in order to isolate X_s and X_d enhanced samples.

To determine the signal yields within each final state, both analyses perform an unbinned maximum-likelihood fit to the $B^\pm$ invariant-mass distributions of all four subsamples simultaneously. Careful attention has been made to account for all potential sources of background and to include appropriate lineshapes for each within the global likelihood. The resulting best fit to the four invariant-mass distributions of analysis (B) are shown in Fig. 1. Clear signal peaks are seen in both the $[\pi^+\pi^-]_D$ (Figs. 1(a) and 1(b)) and $[K^+K^-]_D$ (Figs. 1(c) and 1(d)) final states, constituting the first ever observations of these CP modes within the decay $B^\pm \to DK^\pm\pi^+\pi^-$. Furthermore, hints of charge asymmetries are also seen between Figs. 1(a) and 1(b) and Figs. 1(c) and 1(d), respectively.

The measurements of R_{CP^+} and A_{CP^+} for both analysis (A) and (B) are quoted in Table 2 [7, 8]. In addition to values of A_{CP^+} specific to $B^\pm \to DX_s^\pm$, results of A_{CP^+} corresponding to the reflection

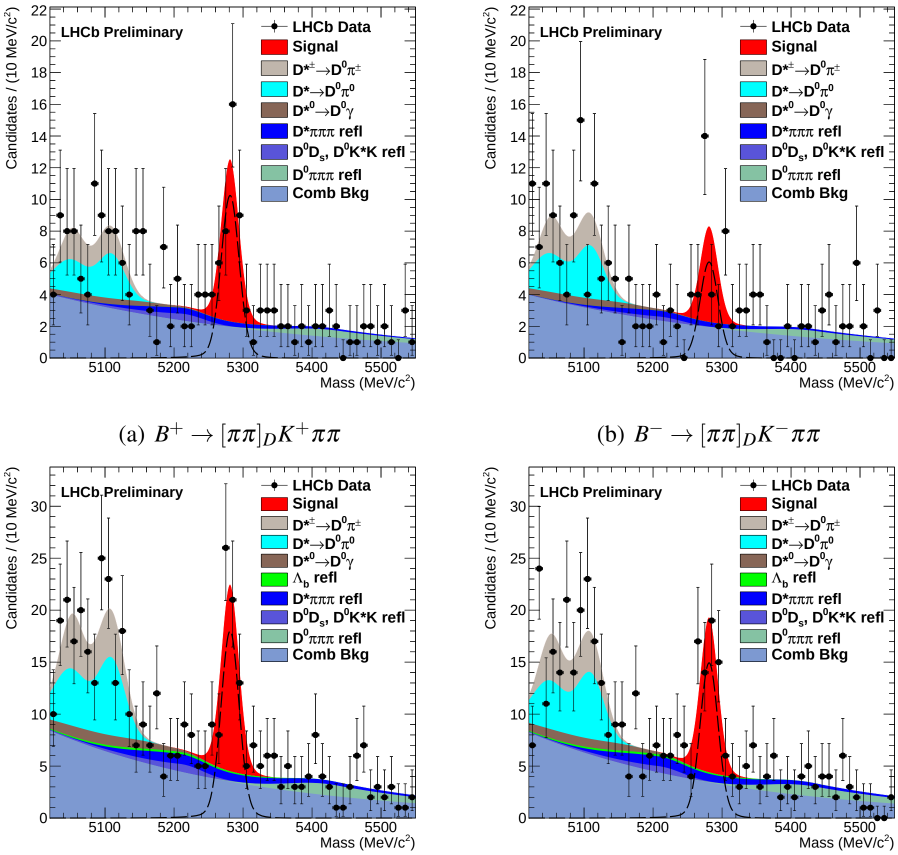

(a) $B^+ \to [\pi\pi]_D K^+\pi\pi$

(b) $B^- \to [\pi\pi]_D K^-\pi\pi$

(c) $B^+ \to [KK]_D K^+\pi\pi$

(d) $B^- \to [KK]_D K^-\pi\pi$

Figure 1: $B^\pm \to D_{CP+} K^\pm\pi^+\pi^-$ invariant mass distributions, separated by charge and D_{CP+} final state.

modes $B^\pm \to DX_d^\pm$ are also given. To distinguish them, these two quantities are denoted as A^s_{CP+} and A^d_{CP+}, respectively. The results for analysis (A) are also world best measurements, with a non-zero value of A^s_{CP+} observed in excess of 4.5 σ.

X	R_{CP^+}	$A^s_{CP^+}$	$A^d_{CP^+}$
$h^\pm$	$1.007 \pm 0.038 \pm 0.012$	$0.145 \pm 0.022 \pm 0.010$	$-0.02 \pm 0.02 \pm 0.01$
$h^\pm\pi^+\pi^-$	$0.95 \pm 0.11 \pm 0.02$	$-0.14 \pm 0.10 \pm 0.01$	$-0.018 \pm 0.018 \pm 0.010$

Table 2: Measurements of the GLW observables R_{CP^+}, $A^s_{CP^+}$ and $A^d_{CP^+}$ for $B^\pm \to DX^\pm$, $X = h^\pm$ and $X = h^\pm\pi^+\pi^-$ where h is either a kaon or pion.

4. Time Independent Measurements : ADS Method

Optimal sensitivity to γ is achieved when the interference between $B^\pm \to \overline{D^0}X_s^\pm$ and $B^\pm \to D^0X_s^\pm$ is maximal. Ref. [6] demonstrates that the interference in such decays can be maximised by considering a D final-state accessible via either a Cabibbo Favoured or a Doubly Cabibbo Suppressed decay, such as $K^\pm\pi^\mp$ and requiring the charge of the kaon be opposite to that of the final state X_s. These decays, $B^\pm \to [K^\mp\pi^\pm]_D X_s^\pm$, are referred to as suppressed ADS (sADS) modes and are highly sensitive to γ. The like-sign combinations, $B^\pm \to [K^\pm\pi^\mp]_D X_s^\pm$, are referred to as favoured ADS (fADS) modes and, while they have reduced sensitivity to γ, act as an important normalisation for the sADS modes. The branching fraction of the sADS mode in the case of $X_s = K$ is $\mathscr{O}(10^{-7})$, and until now no 5σ observation has been made.

A search for the $B^\pm \to [K^\mp\pi^\pm]_D K^\pm$ sADS signal has been performed at LHCb as an extension of analysis (A) described in Sec. 3. Here, events in both the sADS and fADS final states, separated by charge, are considered within a full fit simultaneously with the four GLW final states. The resulting best fit to the sADS datasets are show in Fig. 2. The red peaks in Figs.2(a) and 2(b) correspond to the sADS signal, which is observed for the first time with a significance of $\sim 10\sigma$.

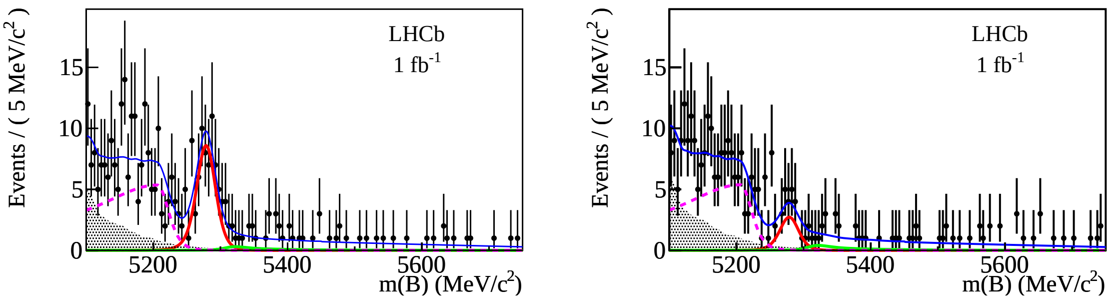

(a) $B^+ \to [K^-\pi^+]_D K^+$ (b) $B^- \to [K^+\pi^-]_D K^-$

Figure 2: The B invariant mass distributions for (a) positively- and (b) negatively-charged candidates within the $B^\pm \to [K^\mp\pi^\pm]_D K^\pm$ sADS final state. Clear signal peaks (red) are visible, while the contributions from residual $B^\pm \to [K^\mp\pi^\pm]_D \pi^\pm$ (green) and low-mass sources are also accounted for.

Measurements of two associated CP observables are performed for both the $B^\pm \to [K^\mp\pi^\pm]_D K^\pm$ and $B^\pm \to [K^\mp\pi^\pm]_D \pi^\pm$ sADS signals. Both observables have dependance on the ratio of partial widths for the sADS and fADS final states. For the modes $B^\pm \to [K^\mp\pi^\pm]_D K^\pm$ this quantity is

$$\mathscr{R}_s^\pm = \frac{\Gamma([K^\mp\pi^\pm]_D K^\pm)}{\Gamma([K^\pm\pi^\mp]_D K^\pm)}. \tag{4.1}$$

The first observable is then the charged-averaged ratio of sADS over fADS

$$R^s_{ADS} = \frac{1}{2}(\mathscr{R}_s^+ + \mathscr{R}_s^-) \tag{4.2}$$

and the second is the CP asymmetry

$$A^s_{ADS} = \frac{\mathscr{R}_s^- - \mathscr{R}_s^+}{\mathscr{R}_s^- + \mathscr{R}_s^+}. \tag{4.3}$$

An equivalent set of observables is also accessible for the modes $B^\pm \to [K^\mp\pi^\pm]_D \pi^\pm$; R^d_{ADS} and A^d_{ADS}. Table 3 quotes the results obtained. A large negative value of A^s_{ADS} is found with a significance of 4σ. When combined with the analysis (A) GLW measurements, CP violation is observed for the first time in $B^\pm \to DK^\pm$ decays with a significance of 5.8σ. Furthermore, for the first time an asymmetry of 2.4σ significance is observed in the $B^\pm \to [K^\mp\pi^\pm]_D \pi^\pm$ sADS mode [7].

(%)	$X_s = K$	$X_d = \pi$
R_{ADS}	$1.52 \pm 0.20 \pm 0.04$	$0.410 \pm 0.025 \pm 0.005$
A_{ADS}	$-52 \pm 15 \pm 2$	$14.3 \pm 6.2 \pm 1.1$

Table 3: Measured values of R_{ADS} and A_{ADS} in % for both $B^\pm \to [K^\mp\pi^\pm]_D K^\pm$ and $B^\pm \to [K^\mp\pi^\pm]_D \pi^\pm$ sADS modes.

5. Time-Dependent Measurements

Complementary to performing time-integrated measurements with $B^\pm \to DX_s^\pm$ decays, is to consider the decay $B_s^0 \to D_s K$ within a time-dependent analysis. Such an analysis benefits enormously from the excellent proper time resolution achievable at LHCb, provided by the high precision vertex and tracking systems. While the statistics within the 2011 dataset prevent a measurement of γ being made through this mode, important complementary measurements have been performed. Firstly, a useful demonstration of the flavour tagging performance has been conducted through a high precision measurement of Δm_s with the reflection mode $B_s^0 \to D_s\pi$ [9]. Secondly, measurements of the absolute branching fractions of both $B_s^0 \to D_s K$ and $B_s^0 \to D_s\pi$ have also been performed [10], utilising an earlier LHCb measurement of the ratio of hadronisation fractions, f_s/f_d [11]. All three measurements, summarised in Table 4, have significantly more precision than current world averages.

Measurement	Result	Unit	Integrated Lumi. (pb^{-1})
Δm_s	$17.725 \pm 0.041 \pm 0.026$	ps^{-1}	340
$\mathscr{B}(B_s^0 \to D_s^-\pi^+)$	$(1.90 \pm 0.12 \pm 0.13^{+0.12}_{-0.14}) \times 10^{-4}$	a.u.	370
$\mathscr{B}(B_s^0 \to D_s^\mp K^\pm)$	$(2.95 \pm 0.05 \pm 0.17^{+0.12}_{-0.14}) \times 10^{-3}$	a.u.	370

Table 4: Measured of the quantities Δm_s, $\mathscr{B}(B_s^0 \to D_s^-\pi^+)$ and $\mathscr{B}(B_s^0 \to D_s^\mp K^\pm)$ performed. The amount of integrated luminosity considered in each respective study is also stated.

References

[1] J. Charles *et al.* [CKMfitter Group], Eur. Phys. J. C **41** (2005) 1 [arXiv:0406184[hep-ph]].

[2] R. N. Cahn, Rev. Mod. Phys. **68** (1996) 951.

[3] The LHCb Collaboration, arXiv:0912.4179 [hep-ex].

[4] M. Gronau and D. London, Phys. Lett. B **253** (1991) 483.

[5] M. Gronau and D. Wyler, Phys. Lett. B **265** (1991) 172.

[6] D. Atwood, I. Dunietz and A. Soni, Phys. Rev. Lett. **78** (1997) 3257 [arXiv:9612433[hep-ph]].

[7] R. Aaij *et al.* [LHCb Collaboration], Phys. Lett. B **712** (2012) 203 [Erratum-ibid. B **713** (2012) 351] [arXiv:1203.3662 [hep-ex]].

[8] The LHCb Collaboration, LHCb-CONF-2012-0021, (2012)

[9] The LHCb Collaboration, LHCb-CONF-2011-043, (2011)

[10] R. Aaij *et al.* [LHCb Collaboration], JHEP **1206** (2012) 115 [arXiv:1204.1237 [hep-ex]].

[11] R. Aaij *et al.* [LHCb Collaboration], Phys. Rev. D **85** (2012) 032008 [arXiv:1111.2357 [hep-ex]].